



Thermodynamic Analysis and Comparison of Two Novel Organic Rankine Systems based on Solar Loop Heat Pipe Evaporator

V. Beygzadeh^{a*}, S. Khalil Arya^b, I. Mirzaee^b, G. Miri^c, V. Zare^a

^aDepartment of Mechanical Engineering, Faculty of Engineering, Urmia University of Technology, Iran, *Email: vbeygzadeh@gmail.com

^bDepartment of Mechanical Engineering, faculty of engineering, Urmia University, Urmia, Iran,

^cDepartment of Business Management, National Iranian Oil Refining & Distribution Company, Tehran, Iran,

ARTICLE INFO

Received: 02 May 2018
Received in revised form:
19 Jul 2018
Accepted: 19 Jul 2018
Available online:
05 Dec 2018

Keywords:

Energy efficiency;
exergy efficiency;
SLHPS; solar; ORC;

ABSTRACT

A comprehensive thermodynamic analysis and performance comparison of two solar ORC systems for electricity generation is reported. Energy and exergy analyses are used to characterize the exergy destruction rate in any component and estimate solar ORC systems performance. The systems considered are solar ORC system with single stage turbine and solar ORC system with double stage turbine. A computer simulation program using EES software is developed to model the solar ORC systems. The solar ORC systems provide electricity during the hours of solar radiation. The analysis involves the specification of effects of varying ORC evaporators pinch point, varying ambient temperature and varying ORC turbines inlet pressure on the energetic and exergetic performance of the solar ORC systems. This study shows that the solar ORC system with double stage turbine has the higher performance. The results also showed that the main source of the exergy destruction is the solar loop heat pipe evaporator for both considered systems. Other main sources of exergy destruction are the ORC turbines; and the ORC evaporators for both considered systems.

© 2018 Published by University of Tehran Press. All rights reserved.

1. Introduction

Solar power is pollution free and causes no greenhouse gases to be emitted after installation. Solar thermal energy is a form of energy and a technology for harnessing solar energy to generate thermal energy or electrical energy for use in industry, and in the residential and commercial sectors.

The Organic Rankine Cycle (ORC) is named for its use of an organic, high molecular mass fluid with a liquid-vapor phase change, or boiling point, occurring at a lower temperature than the water steam phase change. The fluid allows Rankine cycle heat recovery from lower temperature sources such as biomass combustion, industrial waste heat, geothermal heat, solar ponds and etc. The low temperature heat is converted into useful work, that can itself be converted into electricity.

The ORC allows power generation at lower capacities and with a lower collector temperature.

A loop heat pipe is a simple device with no moving parts that can transfer large quantities of heat over fairly large distances essentially at a constant temperature. A heat pipe is basically a sealed slender tube containing a wick structure lined on the inner surface and a small amount of fluid at the saturated state [1].

Loop heat pipes are analogous to heat pipes but have the benefit of being capable to provide trustworthy function over lengthy distance and the capability to work versus gravity force. They can carry a large heat load over a long distance. Several layouts of loop heat pipes ranging from, large size loop heat pipes to micro loop heat pipes have been developed and successfully utilized in a broad area of utilizations both ground based and space utilizations.

Iran's unique geographical position means 90% of the country has enough sun to generate solar power 300 days a year. Iran has 520 watts per hour per square meter of solar radiation every day. [2]. Deepak Tiwari et al. [3] carried out Energy and exergy analysis of solar driven recuperated ORC cycle. They showed that overall first law efficiency improves using recuperated ORC. Alireza Javanshir and Nenad Sarunac. [4] carried out Thermodynamic analysis of a simple Organic Rankine Cycle. Arnaud Landelle et al. [5] carried out Organic Rankine cycle design and performance comparison based on experimental database. Soteris A. Kalogirou et al. [6] carried out Exergy analysis on solar thermal systems: A better understanding of their sustainability. Bertrand F. Tchanche et al. [7] Heat resources and organic Rankine cycle machines. They conducted that The nature state and temperature of the heat source significantly influences the choice of the type of organic Rankine cycle machine. Wei He et al. [8] carried out Theoretical investigation of the thermal performance of a novel solar loop heat pipe façade based heat pump water heating system. Xingxing Zhang et al. [9] performed Characterization of a solar photovoltaic/loop heat pipe heat pump water heating system. Xudong Zhao et al. [10] carried out Theoretical investigation of the performance of a novel loop heat pipe solar water heating system for use in Beijing, China.

The loop heat pipes are ideally suited for use in solar systems, which allow solar heat to be

collected and transported to a heat exchanger at the inside of the system.

In the present study, two different types of ORCs using the same solar loop heat pipe evaporator as a common topping cycle are thermodynamically modelled, assessed and compared with energy and exergy analyses. Each module of ORC cycle consists of a solar loop heat pipe evaporator, an ORC evaporator, a turbine, a condenser, an ORC pump and an auxiliary pump.

The primary objective is to improve understanding of this solar ORC systems and proposal a new low cost solar thermal system. The following specific tasks are performed:

- Model and simulate (using EES software) the solar ORC systems.
- Validate each part of the models and simulations.
- Perform energy and exergy analyses of the solar ORC systems to determine the exergy destruction rate of each component and energy and exergy efficiencies of the entire systems.
- Execute a comprehensive parametric study to determine the effect of major design parameters on systems performance.
- Energetic and exergetic performance comparison of two solar ORC systems.

The systems description and assumptions are presented next. Then, systems modeling, results and discussion, and conclusions are presented, respectively.

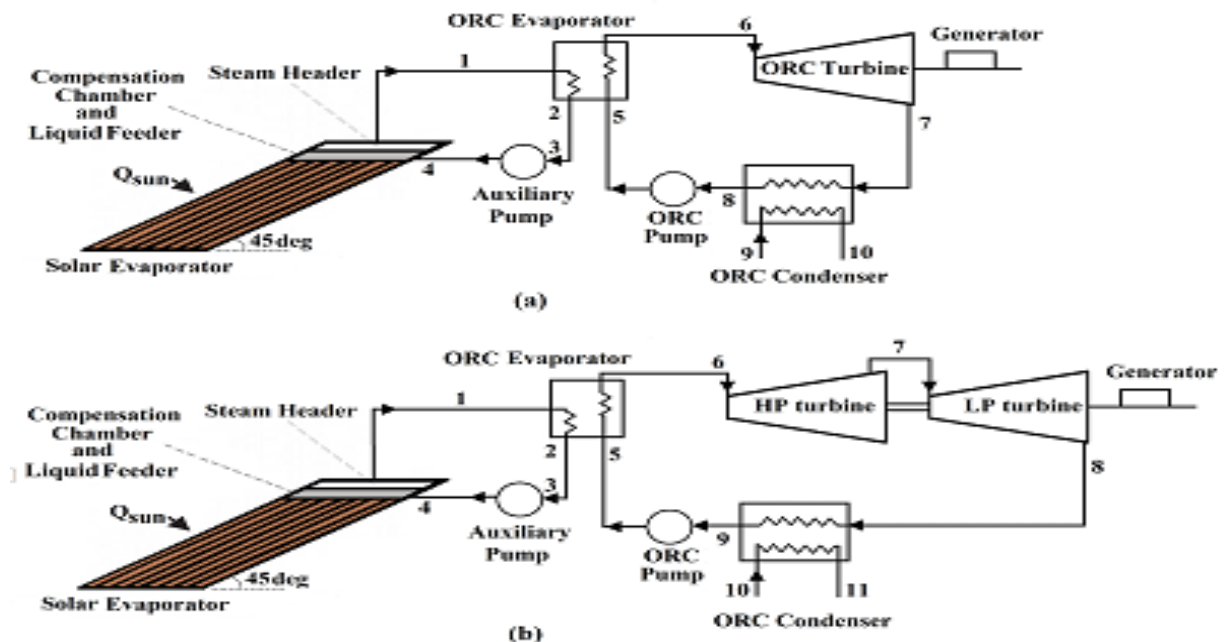


Figure 1. Schematic of the studied systems (a) ORC cycle with single stage turbine, (b) ORC cycle with double stage turbine

2. Materials and Methods

2.1. Systems description

Fig. 1 indicates a schematic of the two ORC systems. Cycle a, comprising a solar loop heat pipe evaporator, an auxiliary pump, an ORC evaporator, a single stage turbine, an electrical generator, a condenser and an ORC pump. Cycle b, comprising a solar loop heat pipe evaporator, an auxiliary pump, an ORC evaporator, a double stage turbine, an electrical generator, a condenser and an ORC pump.

This solar ORC systems use the solar energy under Tabriz spring and summer conditions to evaporate a working fluid (toluene in this study, with the thermodynamic properties listed in Table 1) through the solar loop heat pipe evaporator, which drives ORC evaporator and vaporize ORC cycle working fluid (A typical organic fluid used in ORC is Ethanol, with the thermodynamic properties listed in Table 1).

Properties of toluene (working fluid for SLHPS)		Properties of Ethanol (working fluid for ORC)	
Parameter	Value	Parameter	Value
Chemical formula	C ₇ H ₈	Chemical formula	C ₂ H ₅ OH
Molar mass (kg/kmol)	92.14	Molar mass (kg/kmol)	46.07
Boiling temperature (°C)	111	Boiling temperature (°C)	78.24
Density (kg/m ³)	867	Density (kg/m ³)	789
Freezing temperature (°C)	-95	Freezing temperature (°C)	-114.14
Critical temperature (°C)	318.6	Critical temperature (°C)	240.8
Critical pressure (MPa)	4.126	Critical pressure (MPa)	6.148

Ethanol superheated vapour after leaving ORC evaporator enters to the ORC turbine to produce electricity. The vapor is then condensed in the condenser. The working fluid is then pumped to the ORC evaporator and the cycle is repeated continuously.

The solar loop heat pipe system, is composed of solar evaporator (which is consist of 4177 wicked loop heat pipes), vapour and liquid lines, vapour and liquid headers, compensation chamber, as well as a plate heat exchanger (ORC evaporator).

The loop heat pipes evaporators are located on a low content of Ferro oxide glass plate in parallel lines with a small gap in among. In exploitation, the received solar energy transforms the toluene on the wicks of the loop heat pipes into vapour, which streams along the loop heat pipes to the vapour header, due to the buoyancy of vapour, auxiliary pump pressure and the gravity force created by the altitude discrepancy between the ORC evaporator and the solar evaporator (points 2 and 3 in Fig. 1). The vapour is then hauled to ORC evaporator through the vapour line.

Through the liquid line, the toluene liquid enters the auxiliary pump. The auxiliary pump increases the pressure of SLHPS working fluid and working fluid enters the compensation chamber placed under the vapour header. This amount of liquid is then divided to all loop heat pipes evaporators through a liquid feeder fixed at the over sector of the solar loop heat pipe evaporator, as shown in Fig. 1. The liquid feeder would let the liquid to be descended into the loop heat pipes wicks equally. The schematic of LHP is shown in Fig. 2.

The loop heat pipe system as well as uses a three path structure to supply rapid liquid distribution in the loop heat pipes evaporator wicks, as shown in Fig. 3.

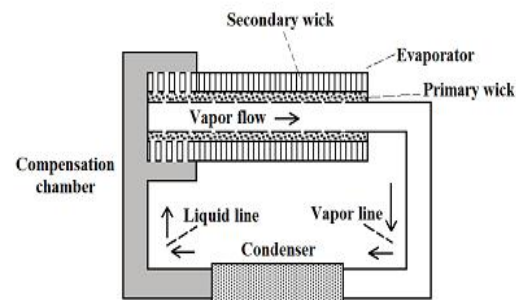


Figure 2. The schematic of LHP

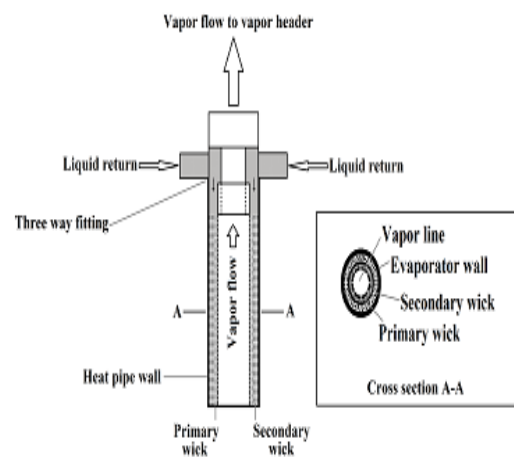


Figure 3. Schematic of three-way feeding and vapour /liquid separation structure

To carry out the thermodynamic analysis and comparison of the proposed systems, the following presumptions are used:

- All the processes are considered to be operating at steady state.
- Heat losses from piping and other components are insignificant.
- Thermal and radiation properties of the solar loop heat pipe evaporator are considered independent of temperature.
- All of the solar loop heat pipe system components are adiabatic except loop heat pipes evaporators.
- The flow regime in the SLHPS is laminar.
- Pressure drop in vapour and liquid headers was neglected.
- Pressure drops in vapour and liquid lines are neglected as they are rather small.
- Pressure drop in compensation chamber was neglected.
- The dead state pressure is 101kPa.
- The dead state temperature is 298.15 K.
- The ambient temperature is 301.15 K.
- Pressure drops in ORC cycles are negligible.
- The average solar radiation during the system operation period of 8:00 until 16:00 was 500 W/m² (under Tabriz spring and summer conditions).
- There is an axisymmetric stream in all the parts of the SLHPS.
- Chemical exergy of components and the kinetic, potential energy and exergy are neglected.

2.2. Thermodynamic modeling

For thermodynamic modeling, the proposed systems (Fig. 1) are divided into two Main parts: solar systems and ORC cycles. The equations developed are programmed using Engineering Equation Solver (EES) software. The input data used in this model are given in Table 2 and Table 3.

Parameter	Value
Turbines efficiency	85%
Pumps efficiency	85%
ORC turbines inlet pressure, kPa	350
ORC pumps inlet pressure, kPa	8
Two stage turbine intermediate pressure, kPa	105
Working fluid	Ethanol
ORC evaporator pinch point, °C	3
ORC evaporator type	Plate heat exchanger
Condenser type	Plate heat exchanger

We specify the input and output enthalpy and exergy streams, exergy destruction rates and energy and exergy efficiencies. The energy balances and governing equations for the main sections of the

proposed systems are described in the following subsections.

Mass, energy and exergy balances for any control volume at steady state operation with negligible potential and kinetic energy changes can be expressed, respectively, by

$$\sum_k \dot{m}_i - \sum_k \dot{m}_e = \frac{dm_{cv}}{dt} \quad (1)$$

$$\frac{dE_{cv}}{dt} = \sum \dot{Q}_{cv} - \dot{W}_{cv} + \sum_i \dot{m}_i h_i - \sum_e \dot{m}_e h_e \quad (2)$$

$$\frac{d\psi_{cv}}{dt} = \sum_i \dot{m}_i \psi_i - \sum_e \dot{m}_e \psi_e + \sum_j (1 - \frac{T_0}{T_j}) \dot{Q}_j - (\dot{W}_{cv} - P_0 \frac{dV_{cv}}{dt}) - \dot{i}_{cv} \quad (3)$$

The specific exergy is given by

$$\psi = (h - h_0) - T_0 (s - s_0) \quad (4)$$

Then the total exergy rate associated with a fluid stream becomes

$$\dot{E} = \dot{m} \psi \quad (5)$$

The relevant mass, energy and exergy balances and governing equations for the main sections of the ORC systems shown in Fig. 1 are described in the following subsections.

In the solar loop heat pipe systems with auxiliary pump, the system heat transfer capacity will be controlled by five limits (sonic, entrainment, viscous, boiling and liquid filling mass limits) the minimum values of these limitations will be the actual retention of the solar loop heat pipe system heat transfer. The values of these limits are related to the thermal properties of the working fluids, loop heat pipes structure and loop heat pipes working conditions.

According to Xingxing Zhang et al. [11], the heat transfer limits of the solar loop heat pipe system is shown in Table 4.

The thermodynamic analysis of the solar loop heat pipe system are presented in this subsection. To model the solar loop heat pipe system, we consider the method used by John A. Duffie et al. [12].

- Solar loop heat pipe evaporator

As shown in Fig. 1, toluene enters the solar loop heat pipe system (solar loop heat pipe evaporator) at point 4 and is heated by the solar loop heat pipe evaporator. The useful heat gained by the working fluid can be written as:

$$\dot{Q}_u = \dot{m}_1 (h_1 - h_4) \quad (6)$$

Where h_1 , h_4 and \dot{m}_1 are the toluene outlet enthalpy, inlet enthalpy and mass flow rate.

The useful power produced by the solar loop heat pipe system is calculated as

$$\dot{Q}_u = A_{SOL,EVA} F_R (S - U_l (T_4 - T_{amb})) \quad (7)$$

Where T_{amb} is the ambient temperature, $A_{SOL,EVA}$ is the solar loop heat pipe evaporator effective area and can be expressed as

$$A_{SOL,EVA} = 0.75 \times N_{LHP} \pi D_o L_e \quad (8)$$

And the F_R is heat removal factor which is around 0.83 for this case and U_l is the overall solar evaporator heat loss coefficient.

Solar evaporator length, (m)	1.5
LHPs evaporators length, (m)	1.5
LHPs wicks length, (m)	1.5
Solar evaporator slope	45°
Overall heat loss coefficient from LHP to ambient (kW/m^2)	0.005
Liquid filling mass, (kg)	3.806
Overall heat loss coefficient from LHP fluid to ambient (kW/m^2)	0.0045
Critical radius of bubble generation for toluene, (m)	0.00000007
Solar evaporator heat removal factor	0.83
LHPs material	Black Nickel
Solar evaporator to heat exchanger height difference	1
Solar evaporator optical efficiency	0.8736
SLHPS heat exchanger height, (m)	2
SLHPS condensers length, (m)	2
Solar system operating temperature range	100-127 °C
LHPs type	Mesh screen
number of LHPs	4177
Thickness of LHPs wicks, (m)	0.0075
LHPs porosity	0.64
Thickness of LHPs secondary wicks, (m)	0.005
Internal diameter of LHPs, (m)	0.049
Thickness of LHPs primary wicks, (m)	0.0025
Effective diameter of wicks pores, (m)	0.1111
External diameter of LHPs evaporators, (m)	0.05
Number of wicks pores	9
Internal diameter of LHPs wicks vapour lines (m)	0.041
SLHPS Vapour header material	Black Nickel
ORC evaporator conductivity, ($W/m.K$)	16
SLHPS vapour line material	Cast iron
SLHPS liquid line material	Cast iron
Thermal conductivity of evaporator wall, ($W/m.K$)	91
Thermal conductivity of evaporator wick, ($W/m.K$)	91

LHPs walls thickness, (m)	0.001
SLHPS vapour line diameter, (m)	0.6
Solar evaporator vapour pressure drop, (kPa)	7
SLHPS liquid line diameter, (m)	0.5
SLHPS liquid line length (m)	4
SLHPS vapour line thickness, (m)	0.002
Solar evaporator liquid pressure drop, (kPa)	4
Low content of Ferro oxide glass transmission factor, (τ)	0.91
Black nickel absorption factor (α)	0.96
ORC evaporator (SLHPS condenser) vapour pressure drop, (kPa)	5
SLHPS liquid line thickness, (m)	0.002
ORC evaporator (SLHPS condenser) liquid pressure drop, (kPa)	1
SLHPS vapour line Length, (m)	3
SLHPS average stream speed, (m/s)	50
Gravity effect pressure, (kPa)	+14.936

Entrainment limit \dot{Q}_{EL} (kW)	1595
Viscous limit \dot{Q}_{VL} (kW)	31912
Sonic limit \dot{Q}_{SL} (kW)	192125
Boiling limit \dot{Q}_{BL} (kW)	703906
Filled liquid Mass limit \dot{Q}_{FL} (kW)	597.367

In Eq. (7), radiation flux absorbed by the solar loop heat pipe evaporator is calculated as:

$$S = \eta_{LHP} G_b \quad (9)$$

Where G_b is the solar radiation and η_{LHP} is the LHP optical efficiency and defined as:

$$\eta_{LHP} = \tau \alpha \quad (10)$$

Where τ is the low content of Ferro oxide glass transmission factor and α is the black nickel absorption factor.

The energy efficiency of the solar evaporator is expressed as

$$\eta_{en,SOL,EVA} = \frac{\dot{Q}_u}{G_b A_{SOL,EVA}} \quad (11)$$

The exergy of a solar loop heat pipe evaporator is defined as

$$\dot{E}_{SUN} = G_b A_{SOL,EVA} \left(1 + \frac{1}{3} \left(\frac{T_{amb}}{T_{SUN}}\right)^4 - \frac{4}{3} \left(\frac{T_{amb}}{T_{SUN}}\right)\right) \quad (12)$$

Where T_{SUN} is the sun temperature and equals to 4500 K.

The exergy destruction of the solar loop heat pipe evaporator is

$$\dot{I}_{SOL,EVA} = \dot{E}_4 - \dot{E}_1 + \dot{E}_{SUN} \quad (13)$$

- Auxiliary pump

The auxiliary pump work can be expressed using an energy rate balance for a control volume around the auxiliary pump as follows:

$$\dot{W}_{AUX,Pump} = \dot{m}_3(h_4 - h_3) \quad (14)$$

The auxiliary pump exergy balance can be expressed as

$$\dot{I}_{AUX,PUMP} = \dot{E}_3 + \dot{W}_{AUX,Pump} - \dot{E}_4 \quad (15)$$

2.3. Validation of the solar evaporator model

The solar evaporator model is validated against the experimental study by E. Azad [13], as shown in Fig. 4. The model demonstrates good agreement with the experimental work. The little deviation in the simulations as compared to the experimental results is due to the systems modelling conditions (for example, ambient temperature).

2.4. ORC cycle with single stage turbine

The superheated Ethanol vapour leaving the ORC evaporator enters to the ORC cycle to produce electricity. Energy balances and governing equation for all components of ORC cycle with single stage turbine are provided below.

- ORC Turbine

An energy balance for ORC turbine can be written as

$$\dot{W}_{ORC,T} = \dot{m}_6(h_6 - h_7) \quad (16)$$

An exergy balance for the ORC turbine can be expressed as

$$\dot{I}_{ORC,T} = \dot{E}_6 - \dot{E}_7 - \dot{W}_{ORC,T} \quad (17)$$

- Condenser

The Ethanol flow from the turbine enters the condenser. Water enters this condenser at a pressure and temperature of 200kPa and 22.28^oC, respectively. The energy and exergy balances for this component can be expressed, respectively, by

$$\dot{m}_7(h_7 - h_8) = \dot{m}_{COND}(h_{10} - h_9) \quad (18)$$

$$\dot{I}_{COND} = \dot{E}_9 + \dot{E}_7 - \dot{E}_{10} - \dot{E}_8 \quad (19)$$

- ORC pump

The ORC pump work can be expressed using an energy rate balance for a control volume around the ORC pump as follows:

$$\dot{W}_{ORC,P} = \dot{m}_5(h_5 - h_8) \quad (20)$$

The ORC pump exergy balance can be expressed as

$$\dot{I}_{ORC,P} = \dot{E}_8 + \dot{W}_{ORC,P} - \dot{E}_5 \quad (21)$$

2.5. ORC cycle with double stage turbine

In the solar ORC cycle with double stage turbine, the Ethanol steam does not expand to the condenser pressure in a single stage. The Ethanol steam expands through a first stage of turbine (high

pressure stage) to pressure between the ORC evaporator and condenser pressures. After expanding in the first stage of turbine (high pressure stage), the Ethanol steam expands in the second stage of turbine (low pressure stage) to the condenser pressure.

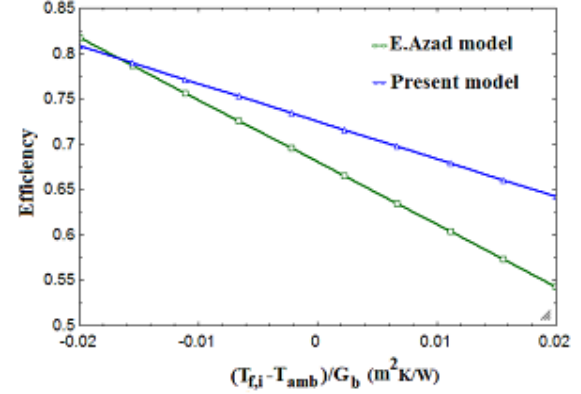


Figure 4. Validation of the solar evaporator model as compared with E. Azad [13]

The superheated Ethanol vapour leaving the ORC evaporator enters to the ORC cycle to produce electricity. Energy balances and governing equation for all components of ORC cycle with double stage turbine are provided below.

- High pressure ORC Turbine

An energy balance for high pressure ORC turbine can be written as

$$\dot{W}_{HPORC,T} = \dot{m}_6(h_6 - h_7) \quad (22)$$

An exergy balance for the ORC turbine can be expressed as

$$\dot{I}_{HPORC,T} = \dot{E}_6 - \dot{E}_7 - \dot{W}_{HPORC,T} \quad (23)$$

- Low pressure ORC Turbine

An energy balance for low pressure ORC turbine can be written as

$$\dot{W}_{LPORC,T} = \dot{m}_7(h_7 - h_8) \quad (24)$$

An exergy balance for the ORC turbine can be expressed as

$$\dot{I}_{LPORC,T} = \dot{E}_7 - \dot{E}_8 - \dot{W}_{LPORC,T} \quad (25)$$

- Condenser

The Ethanol flow from the turbine enters the condenser. Water enters this heater at a pressure and temperature of 200kPa and 22.28^oC, respectively. The energy and exergy balances for this component can be expressed, respectively, by

$$\dot{m}_8(h_8 - h_9) = \dot{m}_{COND}(h_{11} - h_{10}) \quad (26)$$

$$\dot{I}_{COND} = \dot{E}_{10} + \dot{E}_8 - \dot{E}_{11} - \dot{E}_9 \quad (27)$$

- ORC pump

The ORC pump work can be expressed using an energy rate balance for a control volume around the ORC pump as follows:

$$\dot{W}_{ORC,P} = \dot{m}_5 (h_5 - h_9) \quad (28)$$

The ORC pump exergy balance can be expressed as

$$\dot{I}_{ORC,P} = \dot{E}_9 + \dot{W}_{ORC,P} - \dot{E}_5 \quad (29)$$

2.6. Validation of the ORC cycles models

The analysis of the ORC cycles are validated with the literature review, as shown in Table 5.

Literature review	Present study
ORC cycles efficiency: 5.73-25.79%	ORC cycles efficiency: 12.53- 12.63%

The energy efficiency of the ORC systems is defined as

$$\eta_{en} = \frac{\dot{W}_{Net,T}}{G_b A_{SOL,EVA}} \quad (30)$$

The exergy efficiency of the ORC system is defined as

$$\eta_{ex} = \frac{\dot{W}_{Net,T}}{\dot{E}_{SUN}} \quad (31)$$

Here, \dot{E}_{SUN} is the total inlet exergy to the ORC system.

1. Results & Discussion

The solar ORC systems was analyzed using the above equations noting that the environment reference pressure and temperature are 101kPa and 298.15K, respectively. The energy analysis results are summarized in Table 6 and Table 7. The energy analysis shows the energy transfer of each component of the proposed systems and the energy efficiency of the solar ORC systems.

The exergy analysis results are summarized in Table 8 and Table 9, and show that the highest exergy destruction rate happens in the solar loop heat pipe evaporator for both considered systems. As showed above, the major source of exergy destruction is the solar loop heat pipe evaporator and, thus, it needs precise design to improve its performance.

Solar evaporator useful energy	266.5 kW
Condenser energy flow	220.2 kW
ORC evaporator energy flow	266.5 kW
ORC turbine net power	46.22 kW
ORC pump input power	0.1281 kW
Auxiliary pump input power	0.001413 kW
ORC cycle efficiency	12.53%

Solar evaporator useful energy	266.5 Kw
Condenser energy flow	219.9 kW
ORC evaporator energy flow	266.5 kW
ORC turbine net power	46.6 kW
ORC pump input power	0.1281 kW
Auxiliary pump input power	0.001413 kW
ORC cycle efficiency	12.63%

Solar evaporator exergy destruction rate	278.7 kW
ORC evaporator exergy destruction rate	2.931 kW
ORC turbine exergy destruction rate	8.177 kW
ORC pump exergy destruction rate	0.01919 kW
Condenser exergy destruction rate	1.73 kW
Auxiliary pump exergy destruction rate	0.0002096kW
ORC cycle efficiency	13.75 %

3.1. Effect of varying ORC evaporator pinch point on ORC systems performance

Fig. 5 shows the variation with ORC evaporator pinch point temperature of the energy efficiency and exergy efficiency. As shown in this figure, increasing ORC evaporator pinch point temperature reduces the heat flow of the ORC evaporator. When the pinch point temperature increases, the heat absorbed by the ORC evaporator decreases so the utilization of this energy decreases, hence the enthalpy of the Ethanol vapour in the ORC evaporator decreases, which reduces the heat flow and eventually leads to a decrease in the energy and exergy efficiencies of the ORC systems.

3.2. Effect of varying ambient temperature on ORC systems performance

Fig.6 shows the variation of energy efficiency and exergy efficiency with ambient temperature. As can be seen, increasing ambient temperature, increases the energy and exergy efficiencies of the proposed systems, due to an increase in the ambient temperature, decreases the solar evaporator heat losses and exergy destruction rate.

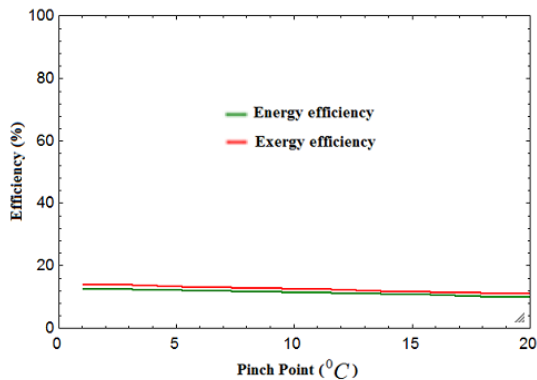
3.3. Effect of varying turbine inlet pressure on ORC systems performance

Fig.7 shows that an increase in turbine inlet pressure enhances the performance of the ORC systems.

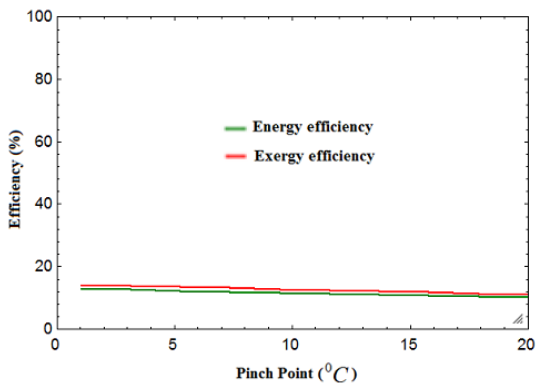
When the turbine inlet pressure increases, the system total irreversibility decreases so the heating load and net power output of the systems increases,

hence the small temperature difference between the fluid streams improves the system's performance.

Solar evaporator exergy destruction rate	278.7 kW
ORC evaporator exergy destruction rate	2.931 kW
ORC turbine exergy destruction rate	7.803 kW
ORC pump exergy destruction rate	0.01919 kW
Condenser exergy destruction rate	1.727 kW
Auxiliary pump exergy destruction rate	0.0002096 kW
ORC cycle efficiency	13.86 %



(a)



(b)

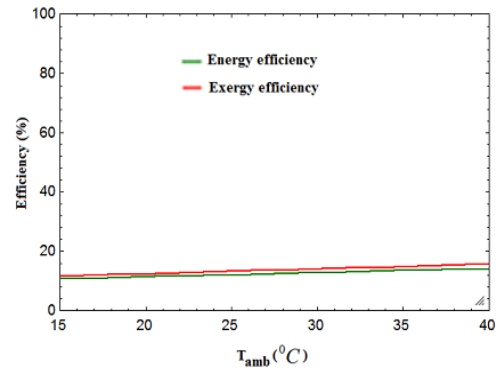
Figure 5. Variation with ORC evaporator pinch point temperature of the energy efficiency and exergy efficiency (a) ORC cycle with single stage turbine, (b) ORC cycle with double stage turbine

4. Conclusions

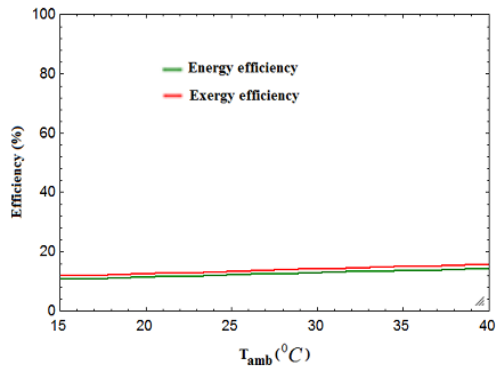
In this study, the steady state thermodynamic analysis and energetic and exergetic performance comparison of two solar ORC systems for electricity generation aims is conducted under Tabriz hot seasons conditions.

The major aim of this study is the finding, expansion, and modeling of a new solar system

with loop heat pipe solar evaporator and introducing a low cost novel solar thermal system. Loop heat pipe has potential to prevail the difficulties in the conventional solar thermal systems and is expected to be low cost and highly efficiency.



(a)



(b)

Figure 6. Variation with ambient temperature of the energy efficiency and exergy efficiency (a) ORC cycle with single stage turbine, (b) ORC cycle with double stage turbine

The results of thermodynamic analysis showed that the solar ORC cycle with double stage turbine have the higher performance as well as output power in comparison with ORC cycle with single stage turbine which make it a key element of successful mechanical drive or power generation services.

The results also showed that the main source of the exergy destruction is the solar loop heat pipe evaporator for both considered systems. Other main sources of exergy destruction are the ORC turbines; then the ORC evaporators and the ORC condensers for both considered systems.

Very few works have been accomplished in field of solar loop heat pipe systems, there are very opportunities existing for further development, for example, developing new, economically and energy and exergy efficient solar systems using loop heat pipes, optimizing the structural of the

solar system configurations to improve their energy and exergy. The results of this research is useful to understand the performance of the solar loop heat pipe evaporators, create the new layouts related to the design of the solar loop heat pipe systems and promote the solar thermal systems.

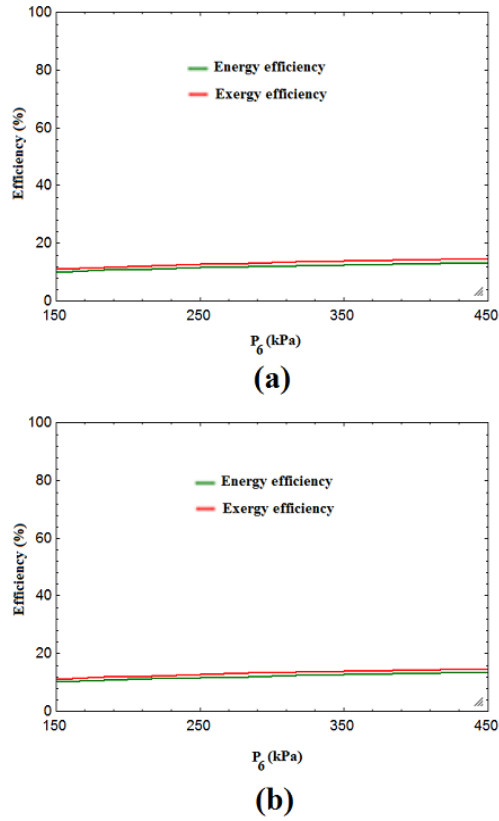


Figure 7. Variation with turbine inlet pressure of the energy efficiency and exergy efficiency (a) ORC cycle with single stage turbine, (b) ORC cycle with double stage turbine

Acknowledgements

The author is thankful to the management and staff of NIORDC for their technical and financial support.

i) Nomenclature

amb	ambient
$A_{SOL,EVA}$	The solar loop heat pipe evaporator area (m ²)
AUX, Pump	Auxiliary pump
CV	control volume
COND	Condenser
D_{ll}	Liquid line diameter
D_{vl}	vapour line diameter
D_o	Loop heat pipes outer diameter
δ_w (m)	Thickness of LHPs wicks

δ_{SW} (m)	Thickness of LHPs secondary wicks
δ_{PW} (m)	Thickness of loop heat pipes primary wicks
E	Energy
\dot{E}	Exergy rate, kW
E _{exit}	exit
F, i	fluid entering solar evaporator
F_R	LHP evaporator heat removal factor
G_b	solar radiation, W/m ²
h	specific enthalpy (kJ/kg)
HPORC, T	high pressure ORC turbine
i	inlet
\dot{I}	Exergy destruction rate (kW)
LPORC, T	low pressure ORC turbine
LHP	loop heat pipe
L_{ll}	Liquid line length
L_{vh}	Vapour header length
L_{vl}	Vapour line length
L_e	Solar evaporator length
\dot{m}	Mass flow rate (kg/s)
m_f (Kg)	solar evaporator liquid filling mass
N_{LHP}	number of loop heat pipes
ORC, P	ORC pump
ORC, T	ORC turbine
(N_p)	Number of wicks pores
P	pressure (kPa)
\dot{Q}	Heat rate, kW
\dot{Q}_{FL} (kW)	Filled liquid Mass limit
\dot{Q}_{SL} (kW)	Sonic limit
\dot{Q}_{EL} (kW)	Entrainment limit
\dot{Q}_{BL} (kW)	Boiling limit
\dot{Q}_{VL} (kW)	Viscous limit
s	specific entropy (kJ/kg-K)
SLHPS	solar loop heat pipe system
SOL, EVA	solar loop heat pipe evaporator
S	radiation absorbed by the solar LHP evaporator
SUN	Sun
T_{SUN}	Sun temperature (K)
T	temperature ⁰ C or K
t	time
u	useful
U_l	Overall heat loss coefficient from LHP to ambient, kW/m ² K
V	Volume
\dot{W}	Work rate, Kw
$\dot{W}_{Net,T}$	Turbine work rate, Kw

η_{ex}	Exergy efficiency
η_{en}	Energy efficiency
ψ	Specific exergy, kJ/kg
η_{LHP}	LHP optical efficiency
τ	Transmission factor
α	Absorption factor

References

- [1]Yunus A. Cengel. (2003). HEAT TRANSFER A Practical Approach. McGraw-Hill.
- [2]Iran Renewable Energy and Energy Efficiency Organization Annual report, 2010-2017.
- [3]Deepak Tiwari, Ahmad Faizan Sherwani, Deepali Atheaya, Akhilesh Arora. (2017). Energy and exergy analysis of solar driven recuperated organic Rankine cycle using glazed reverse absorber conventional compound parabolic concentrator (GRACCPC) system. *Solar Energy*, 155, 1431–1442.
- [4]Alireza Javanshir, Nenad Sarunac. (2017). Thermodynamic analysis of a simple Organic Rankine Cycle. *Energy*, 118, 85-96.
- [5]Arnaud Landelle, Nicolas Tauveron, Philippe Haberschill, Rémi Revellin, Stéphane Colasson. (2017). Organic Rankine cycle design and performance comparison based on experimental database. *Applied Energy*, 204, 1172-1187.
- [6]Soteris A. Kalogirou, Sotirios Karellas, Viorel Badescu, Konstantinos Braimakis. (2016). Exergy analysis on solar thermal systems: A better understanding of their sustainability. *Renewable Energy*, 85, 1328-1333.
- [7]Bertrand F. Tchanche, M. Pétrissans, G. Papadakis. (2014). Heat resources and organic Rankine cycle machines. *Renewable and Sustainable Energy Reviews*, 39, 1185–1199.
- [8]Wei He, Xiaoqiang Hong, Xudong Zhao, Xingxing Zhang, Jinchun Shen, Jie Ji . (2014). Theoretical investigation of the thermal performance of a novel solar loop-heat-pipe facade-based heat pump water heating system. *Energy and Buildings*, 77, 180–191.
- [9]Xingxing Zhang, Xudong Zhao, Jihuan Xu, Xiaotong Yu. (2013). Characterization of a solar photovoltaic/loop-heat-pipe heat pump water heating system. *Applied Energy*, 102, 1229–1245.
- [10]Xudong Zhao, Zhangyuan Wang, Qi Tang. (2010). Theoretical investigation of the performance of a novel loop heat pipe solar water heating system for use in Beijing, China. *Applied Thermal Engineering*, 30, 2526-2536.
- [11]Xingxing Zhang, Xudong Zhao, Jihuan Xu, Xiaotong Yu. (2013). Study of the heat transport capacity of a novel gravitational loop heat pipe. *International Journal of Low-Carbon Technologies*, 8, 210–223.
- [12]John A. Duffie, William A. (2013). Beckman. *Solar Engineering of Thermal Processes*. New York: Wiley.
- [13]E. Azad. (2012). Assessment of three types of heat pipe solar collectors. *Renewable and Sustainable Energy Reviews*, 16, 2833– 2838.